Journal of the Energy Institute xxx (xxxx) xxx

Contents lists available at ScienceDirect

Journal of the Energy Institute

journal homepage: www.journals.elsevier.com/journal-of-the-energy-institute

Synergistic effect for co-coking of sawdust and coal blending based on the chemical structure transformation

Linbo Qin [a, b, c, *], Jun Han [a, b, **], Bo Zhao [a, b], Wangsheng Chen [a, b], Yong Wan [c, ***]

[a] Hubei Key Laboratory for Efficient Utilization and Agglomeration of Metallurgic Mineral Resources, Wuhan University of Science and Technology, Wuhan, 430081, PR China
[b] Hubei Provincial Industrial Safety Engineering Technology Research Center, Wuhan University of Science and Technology, Wuhan, 430081, PR China
[c] State Key Laboratory of Geomechanics and Geotechnical Engineering, Institute of Rock and Soil Mechanics, Chinese Academy of Sciences, Wuhan, 430071, China

ARTICLE INFO

Article history:
Received 4 May 2020
Received in revised form
15 June 2020
Accepted 16 June 2020
Available online xxx

Keywords:
Sawdust
Coal blending
Co-coking
Chemical structure
Synergistic effect
In-situ FTIR-MS

ABSTRACT

Biomass was used as additives in coal blending for making coke in terms of widening the alternative raw materials and reducing CO_2 emissions. To obtain the influences of biomass incorporation on the semicoke formation, the chemical structure transformation as well as the gas evolution during sawdust (SD)/coal blending (BC) co-coking were investigated using in-situ Fourier transform infrared spectroscopy coupled with mass spectrometry (In-situ FTIR-MS). Meanwhile, the role of biomass in the semicoke formation was also characterized by several analytical techniques. The transformation of the five main functional groups between SD and BC exhibited the largest difference, and the synergistic effect based on the chemical structure transformation was also proposed for the SD/BC blends co-coking. The synergistic effect based on the chemical structure transformation was divided into two stages during semicoke formation. One stage occurred at 100–280 °C that was assigned to the physical effect that inhibited the BC decomposition. Another stage happened at 280–500 °C that was mainly attributed to the hydrogen transfer that enhanced the aromatization of semi-coke. In addition, it was also noted that the thermoplastic properties decreased proportionately to the quantity of the SD, and the non-agglomeration between BC and SD was clearly observed by SEM.

1. Introduction

Metallurgical coke derived from coal blending coking at temperatures range of 950–1100 °C, acted as a fuel, a reducing agent, and an indispensable support in iron-making process [1]. The coal blending used as the raw material for metallurgy coke making mainly comprised gas coal, 1/3 coking coal, coking coal, lean coal, and fat coal [2]. It was forecasted that the consumption of coal blending in 2020 would arrive at 500 million tons. However, the deposit of coal for coke making was about 276 billion tons, ~27% of the total coal deposits in China [3]. Due to the limited storage and the price increase of the coal, an alternative renewable energy resource, such as biomass, has been used as additives to be added into the coal blending during the coking process [3–7]. However, high volatile matter and oxygen content in the biomass exhibited an significant effect on coke formation, resulted in the decrease of the coke quality [1,2,8–10]. Our previous investigation reported that 5 wt% of sawdust direct incorporation into coking blends did not affect coke quality, but the coke qualities would gradually reduce when the sawdust addition was above 5 wt% [3]. Montiano et al. [8] found that 15 wt% of briquettes containing waste chestnut sawdust could be included in coking blends for metallurgical coke production.

Coal blending used for the coke production should contain certain physicochemical properties which cause these coals to produce gas and tar and coke in two stages during the coking process [11,12]. One stage is the coal particles undergo soften, liquefy, agglomerate, with simultaneous condensation reactions

* Corresponding author. Hubei Key Laboratory for Efficient Utilization and Agglomeration of Metallurgic Mineral Resources, Wuhan University of Science and Technology, Wuhan, 430081, PR China.
** Corresponding author. Hubei Key Laboratory for Efficient Utilization and Agglomeration of Metallurgic Mineral Resources, Wuhan University of Science and Technology, Wuhan, 430081, PR China.
*** Corresponding author.
E-mail addresses: qinlinbo@wust.edu.cn (L. Qin), hanjun@wust.edu.cn (J. Han), ywan@whrsm.ac.cn (Y. Wan).

https://doi.org/10.1016/j.joei.2020.06.003
1743-9671/

which result in the formation of non-volatile semicoke when the coal particles are heated up to 500–550 °C in inert atmosphere [13]. Another stage is the semicoke continues to undergo a series of reactions and produce high-temperature coke with strong mechanical resistance and moderate CO_2 reactivity as the temperature further increases from 500–550 to 950–1100 °C [14]. The semicoke formation stage is a key step for understanding the physicochemical properties of the resultant coke [15,16]. Meanwhile, the optical texture obtained from the semicoke stage is generally persisted in the resultant coke [17]. In fact, aliphatic groups (CH_3, CH_2, CH), aromatic groups (aromatic C=C and C=H), and oxygen-containing groups (hydroxyl, carbonyl, carboxyl and ether) are the most abundant chemical structure in both biomass and coal that are correlated with the CO_2, CO, C_xH_y, tar and coke formation [13,18–20]. Understanding the transformation of these chemical structure can help to optimize the yields and qualities of coke and tar that obtained from the biomass/coal blends co-coking. However, the chemical structure transformation of biomass/coal blends was not discussed for the semi-coke or coke formation. Nevertheless, the chemical structure transformation together with the gas evolution during biomass/coal blends co-coking was not explicitly investigated, especially for the semicoke formation stage.

Solomon [21] studied the coal pyrolysis using fourier transform infrared spectroscopy (FTIR). The gas products were determined by pyrolysis-FTIR, TG-FTIR and pyrolysis-MS [22]. The chemical structure transformation during coal pyrolysis was measured by an ex situ FTIR and nuclear magnetic resonance spectrometry [23]. However, data obtained from above experimental methods could not directly reflect the variations of coal during pyrolysis, resulted in the relationships between the gas evolution and the chemical structure during coal pyrolysis could not discovered. Niu et al. [24] investigated the chemical structure transformation during coal pyrolysis using in-situ transmission FTIR, the thermal behaviour and kinetics of coal based on the chemical structure transformation were obtained, while the gas evolution during coal pyrolysis were not considered. In-situ Fourier transform infrared spectroscopy equipped with a mass spectrometry (In-situ FTIR-MS) was employed to investigate the reaction mechanism by means of measuring the chemical structure transformation as well as the gas evolution during carbon-based materials thermal degradation. Some publications about waste pyrolysis in in-situ FTIR-MS measurement had been reported in our previous work [25,26].

In this paper, co-coking of biomass/coal blends is studied using in-situ FTIR-MS coupled technology. The chemical structure transformation together with the gas evolution during sawdust/coal blends co-coking are also discussed. Meanwhile, the role of biomass in the semicoke formation is also characterized by the Gieseler plastometer, scanning electron microscope (SEM), and fourier transform infrared spectrometer in the attenuated total reflectance mode (FTIR-ATR). The purposes of this study are: 1) to gain the chemical structure transformation of individual biomass/coal and the biomass/coal blends during semicoke formation process; 2) to obtain the synergistic effect mechanism between sawdust and coal blending during semicoke formation process. The result of this study is expected to provide a useful basis for understanding coke formation during biomass/coal blends co-coking.

2. Materials and methods

2.1. Materials

Four different rank coals (gas coal, 1/3 coking coal, coking coal and lean coal) and pine sawdust (SD) were used in this study, as listed in Table S1. Four different rank coals were sampled from a coking plant, Hubei province, China, and the SD was obtained from a furniture factory, Hubei province, China. Before the experiments, coal blending (BC) is prepared according to the ratio: 26 wt% gas coal, 23 wt% 1/3 coking coal, 43 wt% coking coal and 8 wt% lean coal. The BC and the SD are milled to 74–150 μm, and then the BC and SD are uniformly mixed by an I-type drum. The blends of the SD and BC are named as SDBC-5, SDBC-10, SDBC-15 and SDBC-20, inferring that the mass percentage of the SD in the SD/BC blends is 5%, 10%, 15% and 20%, respectively. The characteristics of the BC and SD are listed in Table 1.

2.2. In-situ FTIR-MS analysis

In-situ FTIR experiments are carried out on an FTIR spectrometer (FTIR, Bruker Tensor II) equipped with a Harrick reaction cell. The FTIR spectrometer is used to monitor the chemical structure transformation during SD/BC pyrolysis varied with the temperature. The spectra are recorded under the wavenumber range of 4000–400 cm^{-1} with a resolution of 4 cm^{-1}. The Harrick reaction cell is electrically heated from the room temperature to 500 °C, and the temperature is automatically controlled and monitored by a thermocouple. Meanwhile, a mass spectrometer (Agilent QMS403) is employed to measure the gas evolution profiles that produced from the SD/BC blends pyrolysis in the Harrick reaction cell.

Approximately 50 mg BC, SD or SD/BC blends is placed in the Harrick reaction cell. Prior to experiment, argon with flow rate of 20 ml min^{-1} is introduced into Harrick reaction cell for 30 min to produce the inert atmosphere, and then the FTIR spectra is also measured by the spectrometer when the Harrick reaction cell is heated from 30 °C to 500 °C under a heating rate of 5 °C·min^{-1} during BC, SD or SD/BC blends pyrolysis. Meanwhile, the ions signals of the gas species released from the Harrick reaction cell are also monitored by the on-line MS.

In order to understand the chemical structure transformation during SD/BC blends pyrolysis, curve-fitting analysis of the FTIR spectrum is performed using peak fitting software, which has been detailly discussed in our previous paper [26].

2.3. Gieseler thermoplastic test and semicoke characterization

The Gieseler thermoplastic of the SD/BC blends is performed in a Gieseler plastometer (PL-2006A, China). 5 g samples are heated up from 300 °C to 550 °C under a heating rate of 3 °C·min^{-1}. The thermoplastic parameters such as softening temperature (T_s), resolidification temperature (T_r) and maximum fluidity (ddpm) are obtained from the experiments.

The chemical structure of these semicoke derived from the SD/BC blends pyrolysis under different temperature was analyzed by Fourier Transform infrared spectroscopy (FTIR) in the attenuated total reflectance (ATR) mode. The FTIR-ATR spectra of the semicokes was measured in a Bruker Tensor II spectrometer equipped with a single bounce diamond ATR crystal at a resolution of 4 cm^{-1} with wavenumbers range of 4000–400 cm^{-1}.

In addition, surface morphology of these semicokes obtained from the Gieseler experiments are analyzed by scanning electron microscope (SEM, Mode Sirion-2000).

2.4. TG analysis

The TG experiments are performed on a thermogravimetric analyzer (NETZSCH STA449 F3). About 200 mg BC, SD or SD/BC blends is loaded into an aluminum crucible that placed on the TG furnace. The sample is heated from 50 to 1000 °C with a heating rate (β) of 5 °C·min^{-1} in 200 ml/min argon atmosphere.

Please cite this article as: L. Qin et al., Synergistic effect for co-coking of sawdust and coal blending based on the chemical structure transformation, Journal of the Energy Institute, https://doi.org/10.1016/j.joei.2020.06.003

Table 1
The basic characteristics of BC and SD.

BC	Proximate analysis,%							Sulfur %	Coking index	Plastometer		
	Moisture	Ash		Volatile	Fixed carbon					X	Y	
	1.80	9.35		28.33	60.52			0.56	82	28	15	
	Ash Chemistry,%											
	SiO_2	Al_2O_3	Fe_2O_3	TiO_2	P_2O_5	CaO	MgO	MnO	Na_2O	K_2O	BaO	Basicity index
	47.71	33.44	10.40	1.98	0.27	4.05	0.91	0.06	0.29	0.78	0.11	0.160
SD	Proximate analysis,%							Sulfur %	Coking index	Plastometer		
	Moisture	Ash		Volatile	Fixed carbon					X	Y	
	9.78	0.78		45.09	44.35			0.11	–	–	–	
	Ash Chemistry,%											
	SiO_2	Al_2O_3	Fe_2O_3	TiO_2	P_2O_5	CaO	MgO	MnO	Na_2O	K_2O	BaO	Basicity index
	29.33	7.90	4.57	0.12	2.33	37.20	6.93	0.07	0.34	10.87	0.34	0.127

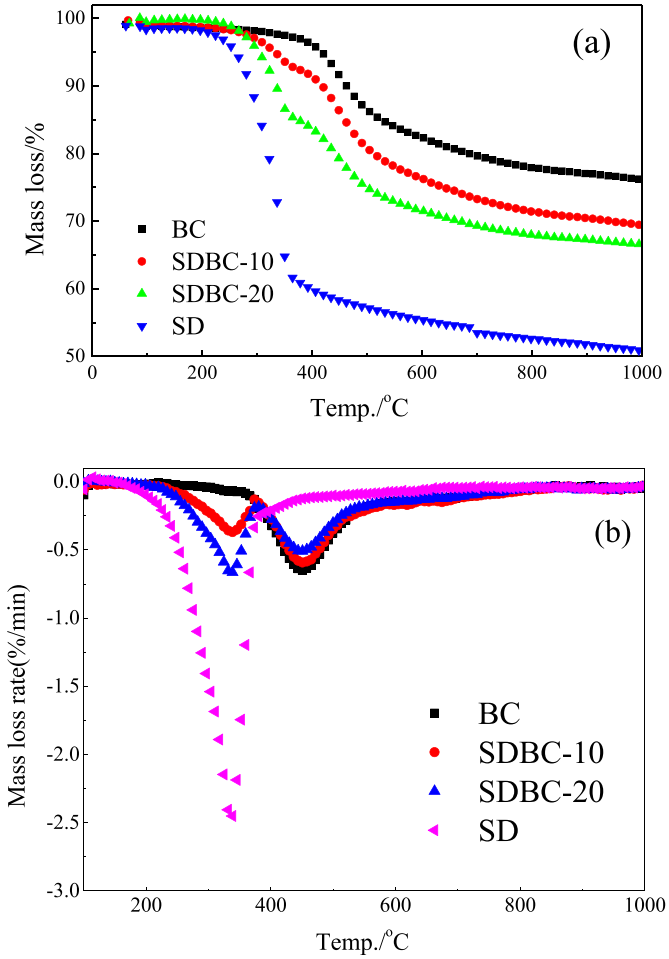

Fig. 1. The mass loss and mass loss rate of the SD, BC, SDBC-10 and SDBC-20 pyrolysis under argon atmosphere at the heating rate of 5 °C·min^{-1}.

3. Results and discussion

3.1. Thermal behavior of SD/BC

Fig. 1 presents the mass loss/mass loss rate of the SD, BC, SDBC-10 and SDBC-20 pyrolysis with a heating rate of 5 °C·min^{-1} in argon atmosphere. It can be seen that an obvious double peak centred at 337 °C are observed under the heating rate of 5 °C·min^{-1} during the SD pyrolysis, as illustrated in Fig. S1. The SD is composed of lignin, cellulose, hemicellulose, and inorganic mineral [20]. It can be induced that the SD pyrolysis exhibits three decomposition stages. The first stage, which exhibits a large amount of mass loss at temperature range of 180–400 °C, indicating the decomposition of the hemicellulose and cellulose [27]. The second stage, occurring between 280 and 450 °C, corresponding to the lignin decomposition [28]. Insignificant mass loss is occurred in the whole temperature zone (Peak 3), which is caused by the release the inorganic mineral. Fig. 1 represents the mass loss/mass loss rate of the BC pyrolysis under a heating rate of 5 °C·min^{-1} in argon atmosphere. The mass loss rate of the BC pyrolysis exhibits two peaks at 300–550 °C and 550–1000 °C, respectively. One peak centred at about 450 °C represents the major stage of the BC pyrolysis, while another peak centred at about 650 °C is assigned to creaking of tar, releasing of the alkali and alkaline earth metals, and aromatization of the semicoke produced from the BC pyrolysis [29]. On the basis of the thermal behaviour of SD and BC pyrolysis that the SD decomposition takes place at 200–400 °C and reaches a maximum of volatile releasing near 340 °C, while the BC starts to decompose when heated to around 400 °C and reaches the maximum of mass loss rate near 450 °C accompanying with more volatile release, as shown in Table 2. Accordingly, the thermal behaviour as well as the chemical structure of the SD and BC differ from each other, which could influence the chemical structure transformation of the SD and BC in different ways.

Table 2
The results of thermoplastic parameters.

Sample	G	T_s/°C	T_f/°C	T_r/°C	P_r/°C	Log(MF)
BC	82	407	445	495	88	3.1
BC+5% SD	82	409	447	492	83	3.0
BC+10% SD	76	412	454	490	78	2.6
BC+15% SD	73	415	457	488	73	2.2
BC+20% SD	71	418	459	487	69	1.6

Fig. 1 also displays the mass loss/mass loss rate of the SD/BC blends (SDBC-10 and SDBC-20) co-pyrolysis. It can be observed that there are two obvious peaks for mass loss rate curve during the SD/BC blends co-pyrolysis. The first peaks centred at 336 °C, 336 °C for the SDBC-10 and SDBC-20 are ascribed to the SD decomposition, while the second peak centred at 450 °C, 449 °C for SDBC-10 and SDBC-20 are mainly assigned to the decomposition of the BC. The mass loss and mass loss rate between experimental values and the calculated values during SD/BC co-pyrolysis under a heating rate of 5 °C·min^{-1} are compared in Fig. 2. It can be seen that the mass loss and mass loss rate obtained from experiments are higher than that of the theoretical results when the temperature range of 240–500 °C. The above phenomena can be induced that the synergistic effect between BC and SD exists during semicoke formation process, and this synergistic effect influences the chemical structure transformation as well as the gas evolution, which will be discussed in section 3.3.

In addition, the influence of the SD addition on thermoplasticity of the SD/BC blends is also probed by Gieseler test, as shown in

Please cite this article as: L. Qin et al., Synergistic effect for co-coking of sawdust and coal blending based on the chemical structure transformation, Journal of the Energy Institute, https://doi.org/10.1016/j.joei.2020.06.003

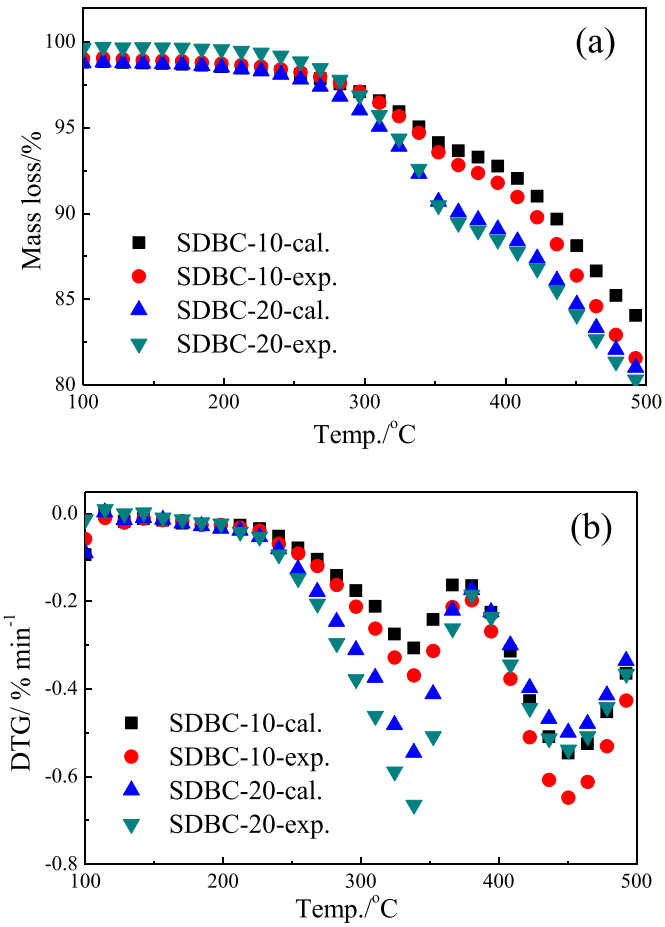

Fig. 2. The comparsion of the conversion rate and reaction rate between experimental values and the calculated values during SD/BC co-pyrolysis.

Table 2. The plastic range of BC is 88 °C. As for the SD/BC blends, the softening temperature of the SD/BC blends increases slightly, while the resolidification temperature of the SD/BC blends decreases significantly. These leads to the reduction of the plastic range as high as 18 °C as the SD addition is increased to 20 wt%. The more significant reduction of the plastic range for the SD/BC blends with 20 wt% SD addition should be attributed to the higher oxygen content and volatile matter in SD [11,30].

3.2. Chemical structures transformation

The mass loss during the SD/BC blends pyrolysis indicates the release of light gas and chemical structure transformation, but the chemical structure transformation does not necessarily result in the mass loss. Therefore, the chemical structure transformation of the five functional groups, including aliphatic C—H, aromatic C—H, aromatic C=C, carbonyls (C=O), and hydroxyls (—OH), which are the most abundant in the chemical structure of the SD and BC, are investigated.

3.2.1. Chemical structures transformation for the individual SD pyrolysis

Fig. 3 depicts the chemical structure transformation during the SD pyrolysis under a heating rate of 5 °C·min^{-1}. As presented in Fig. 3(a), there are five peaks for the aliphatic C—H observed in the 3030–2750 cm^{-1} region during the SD pyrolysis at 100–500 °C, which are attributed to asymmetric methyl stretching (near 3026 cm^{-1}), asymmetric methylene stretching (near 3017 cm^{-1}), aliphatic C—H stretching (near 3006 cm^{-1}), symmetric methyl stretching (near 2990 cm^{-1}), and symmetric methylene stretching (near 2971 cm^{-1}) [31]. The transformation of the aliphatic C—H during the SD pyrolysis exhibits five stages. The quantity of the aliphatic C—H in the first stage (100–160 °C) slowly decreases with the temperature increases due to the evaporation of small molecules with branching chain of polysaccharides in cellulose [32]. However, the transformation of intra- and inter-molecular hydrogen bonds (H—bonds) is a primary reaction that leads to the aliphatic C—H varies slightly at 160–220 °C [33]. The aliphatic C—H at 220–320 °C dramatically decreases due to the depolymerization and fragmentation reaction of cellulose accompanying with the light gas evolution. However, the aliphatic C—H slightly increases at 320–400 °C. The abnormal variation of the aliphatic C—H is assigned to the creaking of the main C=C chain in lignin, which results in the formation of the aliphatic C—H [31]. The decrease of the aliphatic C—H at 400–500 °C is mainly attributed to the cyclization and polycondensation reactions of aromatic polymers in lignin with the release of aliphatic hydrocarbons, as shown in Fig. S2. Fig. 3(b) presents the transformation of the aromatic C=C located at the wavenumber range of 1480–1615 cm^{-1} during the SD pyrolysis under a heating rate of 5 °C·min^{-1}. The bands at 1557, 1539, 1518 and 1505 cm^{-1} are assigned to the aromatic C=C with different rings [31]. The transformation of the aromatic C=C in SD is considerable complex at 100–500 °C since the SD comprises cellulose, hemicellulose and lignin [13]. The aromatic C=C together with the aliphatic C—H in SD slightly decrease below 160 °C due to the light gas evolution in cellulose, as well as water evaporation [32]. The aromatic C=C firstly increases at 160–220 °C and then decreases at 220–280 °C, which may be originated from the removal of substituent groups at aromatic rings in polyxylose [34]. The transformation of the aromatic C=C occurred at 280–380 °C may be caused by the depolymerization and fragmentation reaction, resulted in the formation of monocyclic aromatic hydrocarbons, matching the evolution of benzene (m/z 77, 78) and toluene (m/z 91, 92) monitored by the MS (Fig. S2). The increase of the aromatic C=C between 380 °C and 500 °C is ascribed to cyclization and polycondensation of lignin, accompanying with the formation of H_2 (m/z 2) and CH_4 (m/z 15, 16) [35]. Fig. 3(c) indicates that there are three stages for the transformation of the aromatic C—H during SD pyrolysis. The increase of the aromatic C—H at 100–200 °C is accompanying with the aromatic C=C due to the creaking of bridges of aromatic structure in cellulose, which results in the formation aromatic hydrocarbons. The decrease of aromatic C—H accompanying with gas releasing happened at 200–340 °C is mainly caused by the evolution of monocyclic aromatic hydrocarbons, which is consistent with the variation of the aromatic C=C. However, the aromatic C—H dramatically increases as the temperature increases from 340 to 500 °C due to cyclization and polycondensation [36]. Fig. 3(d) and (e) exhibit the oxygen containing groups such as C=O and —OH varied with temperature during the SD pyrolysis. The C=O evolution in the SD can be separated into four stages at 100–160 °C, 160–260 °C, 260–320 °C and 320–500 °C, respectively. The increase of the C=O at 100–160 °C is attributed to the dewatering of hydrogen bonds. The decrease of the C=O at 160–260 °C is assigned to the degradation of the hemicelluloses since the main ester carbonyl groups in hemicelluloses located at 1635 and 1670 cm^{-1} decrease as the temperature varies from 160 to 260 °C [32]. The peaks attributed to the C=O stretching in phenolic esters at 1699 cm^{-1} and lactones at 1684 cm^{-1} increase at 260–320 °C and then decrease at 320–500 °C. The increase of the C=O at 260–320 °C mostly produces from C—O and —OH groups through dehydration reactions, while the evolution of formaldehyde (m/z 30), acetic acid (m/z 60)

Please cite this article as: L. Qin et al., Synergistic effect for co-coking of sawdust and coal blending based on the chemical structure transformation, Journal of the Energy Institute, https://doi.org/10.1016/j.joei.2020.06.003

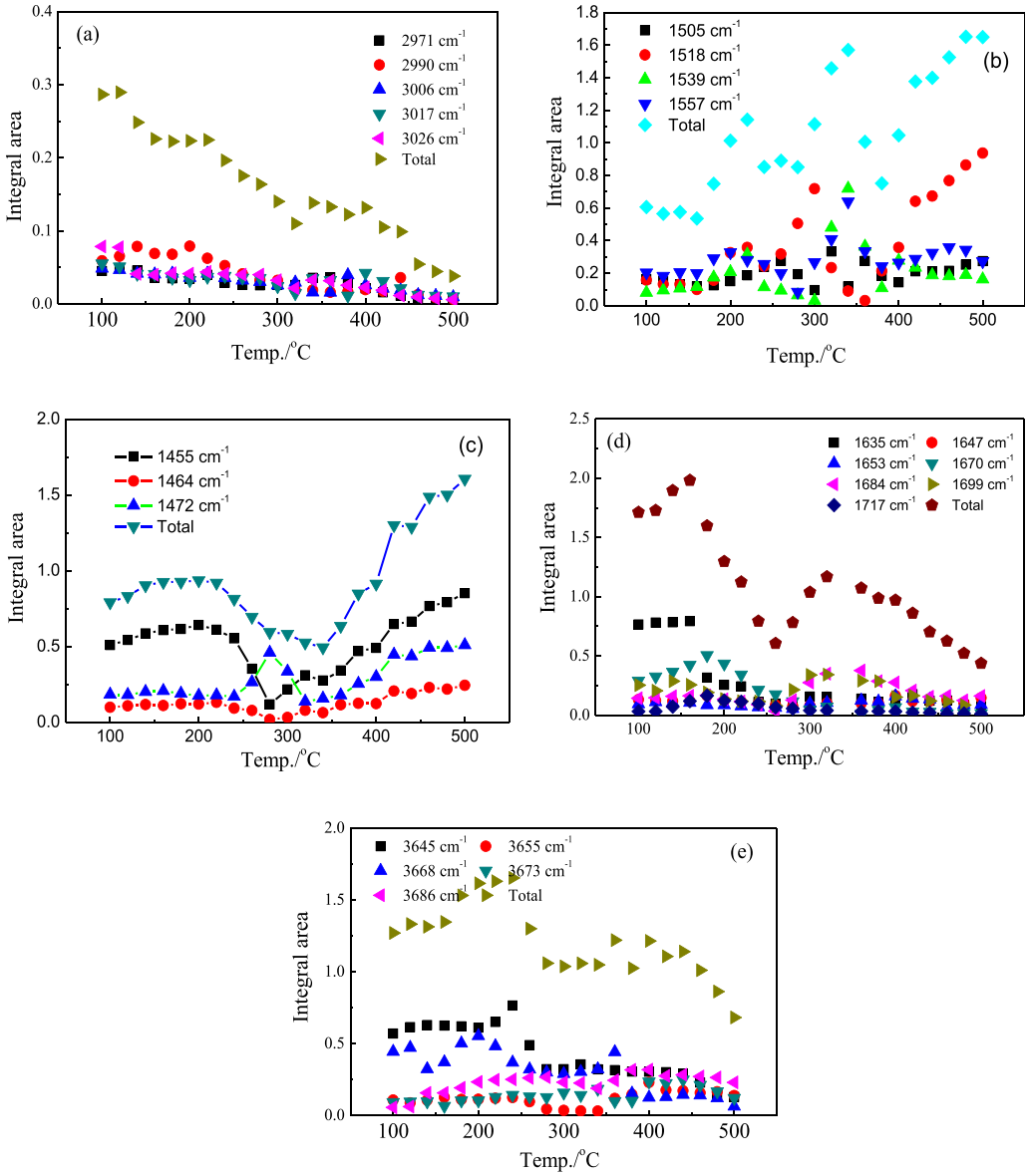

Fig. 3. The chemical structure transformation during the SD pyrolysis with a heating rate of 5 °C·min^{-1}.

and phenol (m/z 94) are contributed for the decrease of the C═O at 260–500 °C, which is also proved by the MS results in Fig. S2. Fig. 3(e) demonstrates that the –OH, especially for the free hydroxyls located at 3668 cm^{-1} increase obviously at 100–240 °C due to the disruption of H-bonds, and then decrease at 240–300 °C, likely due to the dehydration reactions. As temperature further increases from 360 to 500 °C, the –OH sharply decreases accompanying with the H_2O formation.

Thus, the chemical structure transformation during the SD pyrolysis exhibits five stages. The initial stage (happens at 100–160 °C) is assigned to the evaporation of small molecules with branching chain of polysaccharides in cellulose, as well as dewatering of hydrogen bonded water, which increases the aromatic C–H, C═O and –OH, and decrease of aliphatic C–H and aromatic C═C. In the second stage (160–240 °C), the creaking of intra- and inter-molecular hydrogen bonds is the predominated reaction, leads to the increase of aromatic C═C and –OH, and decrease of C═O. The third stage (240–320 °C) are mainly attributed to the dehydration and depolymerization reaction, contributes to the loss of aliphatic C–H, aromatic C–H, and –OH, and formation of C═O and aromatic C═C. The fourth stage occurs between 320 and 400 °C undergoes chain fragmentation primarily to release monomeric phenol units into vapor phase since lignin is a randomly linked phenolic macromolecule [37]. The last stage taking place at 400–500 °C is mainly caused by the deoxygenation and condensation reactions, results in the increase of aromatic C–H and aromatic C═C, and decrease of aliphatic C–H, –OH and C═O.

3.2.2. Chemical structures transformation for the individual BC pyrolysis

Fig. 4 presents the chemical structures transformation during the BC pyrolysis under the heating rate of 5 °C·min^{-1}.The aliphatic C–H transformation during the BC pyrolysis exhibits three stages. The aliphatic C–H existed as bridges in coal structure slightly increase in the initial stage (100–320 °C), which is related to the creaking of $-CH_2-$ [38]. The rapid decomposition of the aliphatic C–H in the BC occurs in the second stage (320–460 °C), which can be evidenced by the evolution of light hydrocarbons, as seen in

Please cite this article as: L. Qin et al., Synergistic effect for co-coking of sawdust and coal blending based on the chemical structure transformation, Journal of the Energy Institute, https://doi.org/10.1016/j.joei.2020.06.003

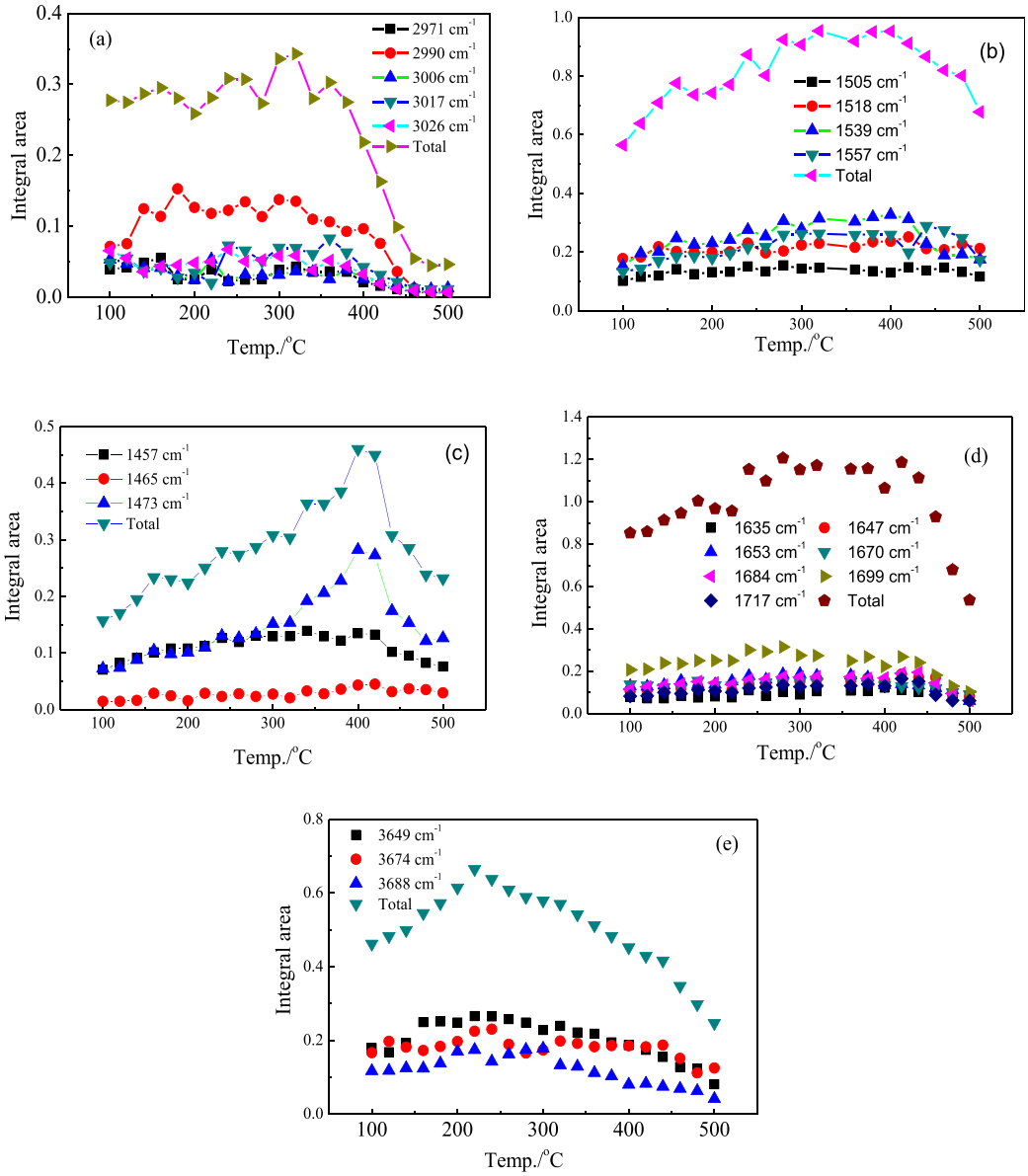

Fig. 4. The chemical structures transformation during the BC pyrolysis under the heating rate of 5 °C·min^{-1}.

Fig. S3. During the third stage (460–500 °C), the total aliphatic C–H for the BC declines slowly with increasing temperature. Fig. 4(b) presents the aromatic C=C transformation during BC pyrolysis firstly increases as the temperature varies from 100 to 380 °C, and then decreases as the temperature further increases from 380 to 500 °C. The increase of the aromatic C=C at 100–380 °C is mainly related to the depolymerization reaction of aromatic polymers with little gas releasing. However, the content of aromatic C=C decreases as the temperature further increases from 380 to 500 °C, accompanying with the evolution of H_2, CH_4, C_2H_4 and toluene due to the creaking and evolution of aromatic rings in BC [25], as shown in Fig. S3. Fig. 4(c) indicates the aromatic C–H during the BC pyrolysis increases with the temperature increases from 100 to 380 °C, and then decreases as the temperature increases from 380 to 500 °C, which is well corresponding to the variation of the aromatic C=C. Fig. 4(d) represents the evolution of the C=O in the BC exhibits three stages at temperatures zone of 100–260 °C, 260–420 °C and 420–500 °C, respectively. The total integral area of the C=O increases up to 260 °C. The peaks at 1699 cm^{-1} and 1653 cm^{-1}, especially at 1699 cm^{-1}, contribute to the increase of the C=O below 260 °C. Niu at al [31]. claimed the increase of the C=O is mainly assigned to the conversion from carbonyl (C–O) to carboxyl (C=O) since the carboxyl in coal blending can be negligible. However, Xiong et al. [39] reported that the dewatering reaction between hydroxyl and carboxyl is not the main contributor to the increase of the 1699 cm^{-1} band. There is no obvious variation observed at 260–420 °C, indicating that temporary stability of C=O in this stage, which is also consistent with the results of Niu et al. [31]. In the third stage, the amount of the C=O dramatically declines in a linear way with the release of acetic acid (m/z 59, 60), as shown in Fig. S3. Fig. 4(e) demonstrates that the –OH increases obviously at 100–220 °C, likely due to the dehydration reactions. As the temperature is further increased from 240 to 500 °C, the –OH sharply decreases accompanying with the H_2O formation, assigned to the elimination of water clusters and the OH in organic structures [40]. The above phenomena should be ascribed to the decomposition pathway of tightly bound hydroxyl tetramers [41]. With the temperature increases, the tetramers convert into smaller

Please cite this article as: L. Qin et al., Synergistic effect for co-coking of sawdust and coal blending based on the chemical structure transformation, Journal of the Energy Institute, https://doi.org/10.1016/j.joei.2020.06.003

groups, and finally decompose into phenol molecular [42], as shown in Fig. S3.

3.2.3. Chemical structures transformation for the SD/BC blends pyrolysis

Figs. 5 and 6 present the chemical structure transformation during the SD/BC blends pyrolysis under the heating rate of 5 °C·min^{-1}. There are four stages for the aliphatic C—H transformation during the SD/BC blends pyrolysis, as shown in Figs. 5(a) and Fig.6(a). The aliphatic C—H in first stage (occurs at 100—240 °C) is related to the creaking of bridges in coal structure with no aliphatic hydrocarbons releasing since the aliphatic C—H during the SD pyrolysis at 100—240 °C exhibits a reduction trendency. The second stage (happens at 240—360 °C) is mainly assigned to the decomposition of SD. The rapid decomposition stages of the aliphatic C—H takes place at 360—420 °C, which is mainly ascribed to the devolatilization with the gas evolution. The transformation of the aliphatic C—H in the last stage (420—500 °C) declines slowly due to the cyclization and polycondensation during semicoke formation process [24]. Figs. 5(b) and Fig.6(b) indicate the transformation of the aromatic C=C during the SDBC-10 and SDBC-20 pyrolysis. It can be seen that there is a similar trendcy for the aromatic C=C transformation between SDBC-10 and SDBC-20. The aromatic C=C firstly increases as the temperature increases from 100 to 280 °C, followed by decreasing at 280—380 °C, and then dramatically increases when the temperature increases from 380 to 500 °C. The increase of the aromatic C=C at 100—220 °C is originated from the creaking of bridges in cellulose structure, while the increase of the aromatic C=C at 220—280 °C is caused by the depolymerization reaction of aromatic polymers since the aromatic C=C decreases at 220—280 °C during the SD pyrolysis and the aromatic C=C derived from the BC pyrolysis increases at 220—280 °C [43,44]. The decrease of the aromatic C=C occurred at 280—380 °C is caused by the evolution of monocyclic aromatic hydrocarbons, which is similar with the SD pyrolysis [45,46]. However, the increase of the aromatic C=C at 380—500 °C is caused by the cyclization, polycondensation and removal of substituent groups at aromatic rings [27]. Figs. 5(c) and Fig.6(c) present the

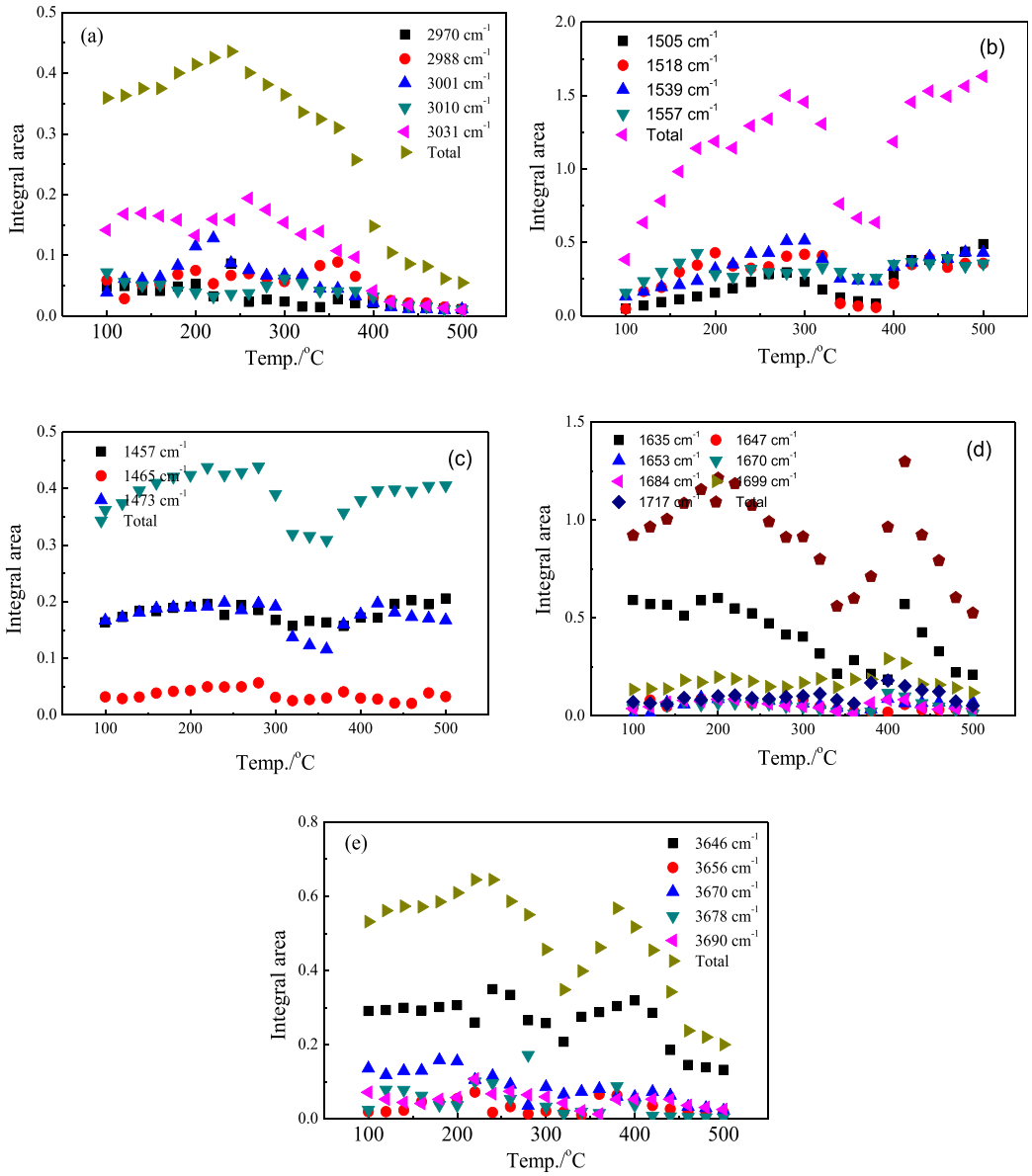

Fig. 5. The chemical structures transformation during the SDBC-10 blends pyrolysis under the heating rate of 5 °C·min^{-1}.

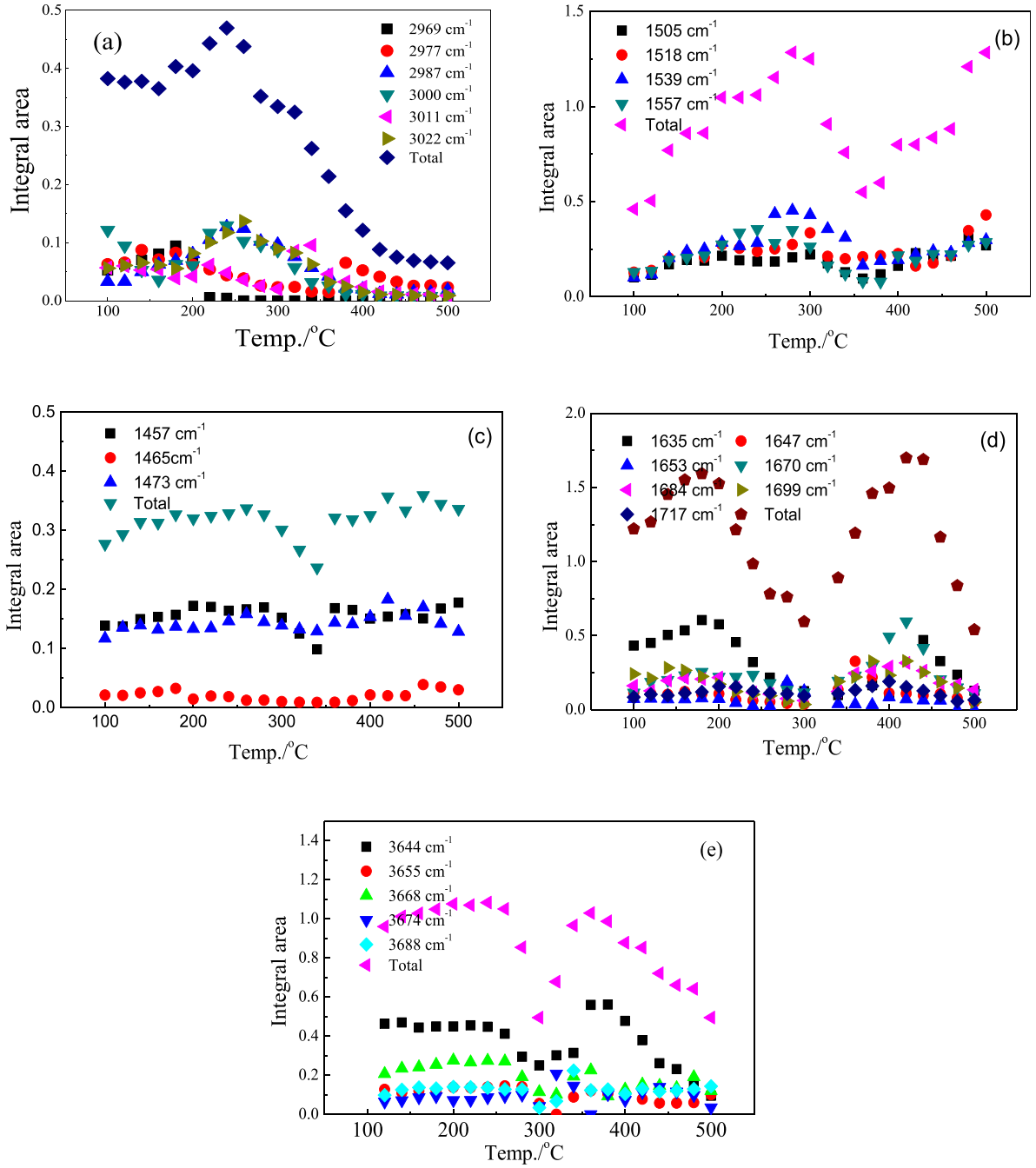

Fig. 6. The chemical structures transformation during the SDBC-20 blends pyrolysis under the heating rate of 5 °C·min^{-1}.

transformation of the aromatic C—H during SDBC-10 and SDBC-20 pyrolysis. The variations of the aromatic C—H during SDBC-10 and SDBC-20 pyrolysis have good correlation with that of the aromatic C═C when the temperature is below 360 °C, while the contents of aromatic C—H vary slightly with the enhancement of temperature when the temperature is above 360 °C. The abnormal variations of the aromatic C—H during SDBC-10 and SDBC-20 pyrolysis at above 360 °C contribute by co-existence of SD and BC since the aromatic C—H derived from the SD pyrolysis increases at above 360 °C, and the aromatic C═C during the BC pyrolysis decreases at above 360 °C [41]. Figs. 5(d) and Fig.6(d) indicate the transformation of the C═O during SDBC-10 and SDBC-20 pyrolysis. Similarly, the C═O transformation in the SDBC-10 and SDBC-20 can be separated into four stages at temperature zone of 100—180 °C, 180—300 °C, 300—420 °C and 420—500 °C, respectively. The increase of C═O at 100—180 °C is attributed to the dewatering of hydrogen bonds. The decrease of C═O at 180—300 °C is assigned to the degradation of hemicelluloses since the main ester carbonyl groups in hemicelluloses located at 1635 and 1699 cm^{-1} decrease with the temperature increases from 180 to 300 °C [32]. The peaks corresponding to the C═O increase at 300—420 °C and then decrease at 420—500 °C. The increase of the C═O at 300—420 °C is likely originated from C—O and —OH through various dehydration reactions, while the evolution of formaldehyde (m/z 30), acetic acid (m/z 60) and phenol (m/z 94) is contributed to the decrease of C═O at 420—500 °C, which is also proved by the MS results in Fig. S4.

Please cite this article as: L. Qin et al., Synergistic effect for co-coking of sawdust and coal blending based on the chemical structure transformation, Journal of the Energy Institute, https://doi.org/10.1016/j.joei.2020.06.003

Figs. 5(e) and Fig.6(e) demonstrate that the −OH increases obviously at 100–240 °C due to the disruption of H-bonds, and then decrease at 240–300 °C due to the dehydration reactions. The increase of −OH at 300–380 °C is likely caused by the synergistic effect between SD and BC, which can be proved by the lower amount of H_2O formation, as compared in Fig. S3 and Fig. S4. As temperature further increases from 380 to 500 °C, the −OH sharply decreases accompanying with the formation of H_2O (m/z 17, 18).

3.3. Synergistic effect based on the chemical structure transformation

In order to further study the synergistic effect mechanism based on the chemical structures transformation during SD/BC blends co-pyrolysis, the normalized integral area of the chemical structures including aliphatic C–H, aromatic C–H, aromatic C=C, C=O, and–OH during SD/BC blends co-pyrolysis are calculated according to the normalized integral area of the chemical structures from the individual BC and SD pyrolysis, as expressed in equation (1):

$$(I_i)_{mixture} = X_{BC} \times (I_i)_{BC} + X_{SD} \times (I_i)_{SD} \quad (1)$$

where $(I_i)_{BC}$, $(I_i)_{SD}$ represents the normalized integral area of the chemical structures varied with the temperature during the individual BC and SD pyrolysis, and X_{BC}, X_{SD} is the mass fractions of the BC and SD in the SD/BC blends, respectively.

Figs. 7 and 8 compare the chemical structures varied with the temperature between the experimental and the calculated results during the SD/BC blends co-pyrolysis. It can be seen that the chemical structures including aliphatic C–H, aromatic C–H, aromatic C=C, C=O, and–OH during the SD/BC blends co-pyrolysis varied with the temperature between the experimental and the calculated results are significantly different, inferring that the interactions between SD and BC exist. Figs. 7(a) and Fig.8(a) indicate that there are obvious differences observed for the aliphatic C–H during SDBC-10 and SDBC-20 pyrolysis in the temperature zones (100–280 °C and 280–500 °C). The normalized integral area of the aliphatic C–H obtained from the experimental results during the SD/BC blends co-pyrolysis at 100–280 °C is much higher than that obtained from the calculated results, indicating that the evolution rate of aliphatic C–H obtained from the experimental results at 100–280 °C is much lower than that obtained from the calculated results, which inferring that the pyrolysis reaction is suppressed at 100–280 °C with less light hydrocarbon formation. Wu et al. [47] claimed that the volatile released from SD may be blocked by the BC and inhibits the SD/BC blends pyrolysis, which is called physical effect. However, the normalized integral area of the aliphatic C–H obtained from the experimental results during the SD/BC blends co-pyrolysis at 280–500 °C is much lower than that obtained from the calculated results, indicating that the evolution rate of aliphatic C–H obtained from the experimental results at 280–500 °C is much higher than that obtained from the calculated results, inducing that the pyrolysis reaction is promoted at 280–500 °C, which is benefitable for the cyclization and polycondensation reaction. The comparisons of the aromatic groups (aromatic C=C and aromatic C–H) varied with the temperature between the experimental values and the calculated values during the SD/BC blends pyrolysis are also represented in Fig. 7(b)–(c) and Fig. 8(b)-(c). It can be seen that there are more aromatic C=C obtained from the experimental results than that obtained from the calculated results, while the normalized integral area of aromatic C–H obtained from the experimental results during the SD/BC blends pyrolysis is much lower than that obtained from the calculated results, indicating that the condensation reactions are promoted due to the synergistic effect between SD and BC, which results in the enhancement of aromatization of semi-coke [48]. It is well known that depolymerization and fragmentation are the two main reactions for semi-coke formation [17]. The liquid intermediates produced from the depolymerization and fragmentation reactions promote the condensation reactions, which cause the condensation structure, such as aromatic C=C, increase remarkably [49]. The dehydration reactions are facilitated in liquid intermediates formation during cellulose pyrolysis. Meanwhile, most of dehydration reactions take place simultaneously with depolymerization and fragmentation, which may be also promoted by the synergistic effect [50,51]. The comparisons of the oxygen containing groups (C=O and −OH) varied with the temperature between the experimental values and the calculated values during the SD/BC blends pyrolysis are also represented in Fig. 7(d)–(e) and Fig. 8(d)-(e). It can be seen that there are three stage differences (ranges of 100–220 °C, 220–380 °C and 380–500 °C) observed between the experimental and calculated results for the normalized integral area of the oxygen containing groups (C=O and −OH). The normalized integral areas of the C=O obtained from the experimental results at temperatures range of 100–220 °C and 380–500 °C are higher than that obtained from the calculated results, while the normalized integral areas of the C=O obtained from the experimental results at temperatures range of 220–380 °C are lower than that obtained from the calculated results. As for the −OH, the normalized integral area of the −OH obtained from the experimental results at temperatures range of 100–220 °C, 220–380 °C and 380–500 °C are lower than that obtained from the calculated results, indicating that the dehydration reactions during the SD/BC blends pyrolysis could be enhanced by the synergistic effect.

The synergistic effect between SD and BC mainly caused by the chemical structure and thermal behavior of the SD and BC. Between 400 and 450 °C, the coal used for coke making begins to soften and provide donatable hydrogens to form liquid intermediates, which favors for the development of plasticity/fluidity [41]. Then, the liquid intermediates recombine with the coal macrostructure to form semicoke. As the temperature further increases to 950 °C, the chemical reactions corresponding to produce coke are dominant and cause a progressive decrease in the fluidity, which results in the aromatic units condensation and coke formation [52]. According to the hydrogen donor theory, richer hydrogen species may produce more mobile hydrogen donor to stabilize radical fragments formed from thermal cracking of coal macrostructure, which is benefitable for the coke formation during the coking process [48]. The volatile with higher H/C from the SD can act as a hydrogen donor that promotes hydrogen transfer reactions, while the volatile with oxygen containing groups from the SD can act as a radical capping that inhibits hydrogen transfer reactions and, consequently, the solvating species generate before coal softening [17]. The recombination of free radicals generated from coals is accelerated, resulting in a less-ordered structure in the semicoke due to cross-linking reactions [49,51,53]. Zhu et al. [54] also reported that the additions of the extracts such as soluble and deposit produced by degradative solvent extraction of biomass at 250–350 °C into the coking coals significantly improved their thermoplastic properties and the coke quality due to the richer hydrogen species in the extracts. The chemical structure of the semicoke derived from these SD/BC blends co-pyrolysis were measured by FTIR-ATR, as presented in Fig. S5. The peaks corresponding to hydroxyls (3720 cm^{-1}), kaolinite (3660, 3620 and 670 cm^{-1}), aliphatic C–H (2920, 2880 cm^{-1}), COOH dimers (2520 cm^{-1}), CO_2 (2260 cm^{-1}), alkyne (2230 cm^{-1}), alkene (1980 cm^{-1}), carbonyl (1730 cm^{-1}), aromatic C–H (1530 cm^{-1}), aromatic C=C (1460 cm^{-1}), phenolic O–H (1260 cm^{-1}), C–O stretching vibration (1060 cm^{-1}) and out-of-plane bending vibration of isolated hydrogen in the benzene ring (900–700 cm^{-1}) in these semicokes derived from SD/BC

Please cite this article as: L. Qin et al., Synergistic effect for co-coking of sawdust and coal blending based on the chemical structure transformation, Journal of the Energy Institute, https://doi.org/10.1016/j.joei.2020.06.003

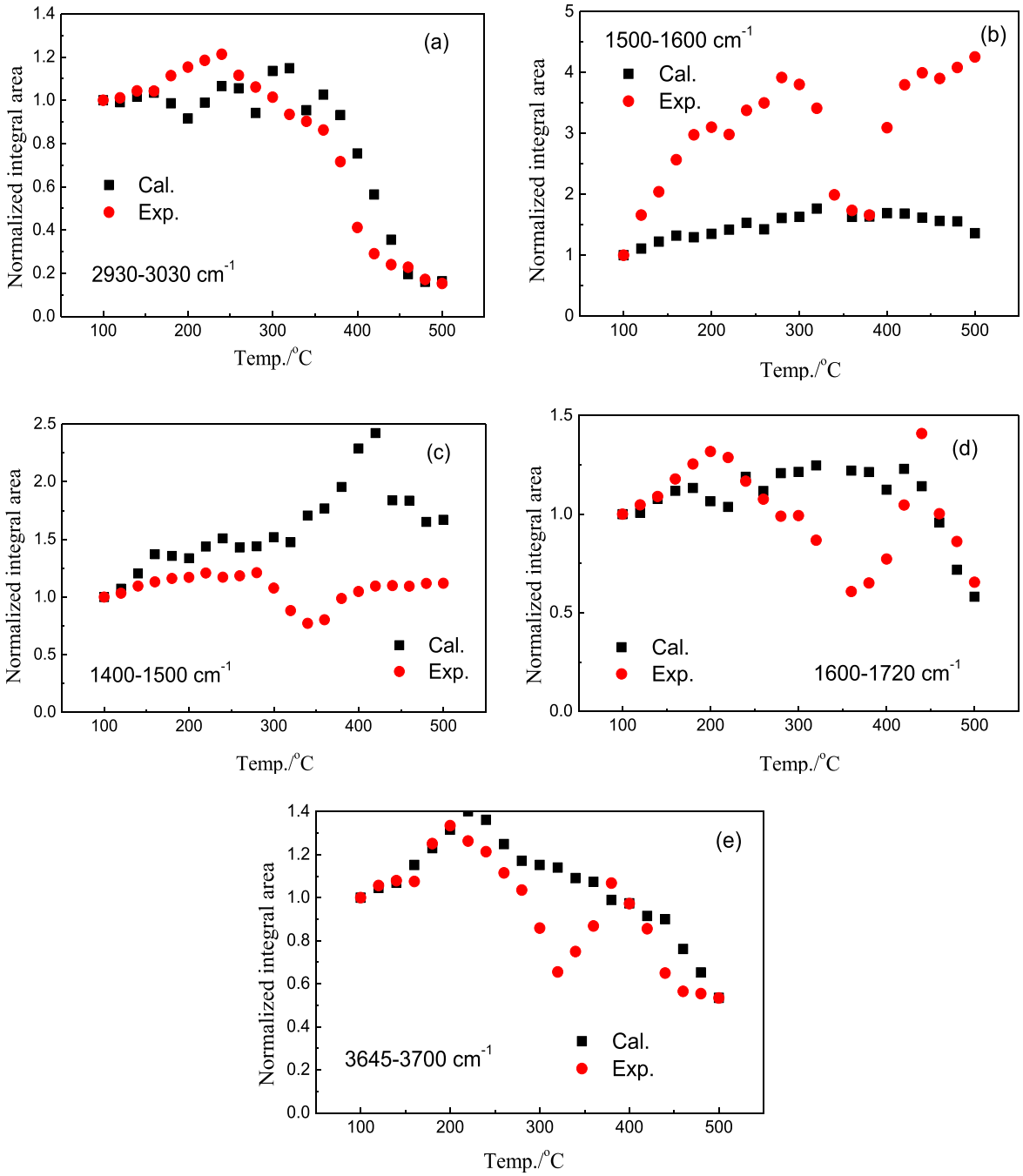

Fig. 7. The functional groups varied with the temperature between the experimental and the calculated results during the SDBC-10 blends co-pyrolysis.

blends co-pyrolysis were observed [55–60]. The increase of C–O stretching vibration (1060 cm^{-1}), carbonyl (1730 cm^{-1}), hydroxyls (3720 cm^{-1}), alkene (1980 cm^{-1}), phenolic O–H (1260 cm^{-1}) and out-of-plane bending vibration of isolated hydrogen in the benzene ring (900–700 cm^{-1}) with the SD incorporation resulted in the decrease of the aromaticity of the semicokes, causing a less poly-aromatic graphite-like structure formation in semicoke [34,39,61]. The SEM images of the semi-coke obtained from BC, SD, SDBC-5, SDBC-10, SDBC-15 and SDBC-20 pyrolysis are shown in Fig. S6. The BC semi-coke displays a strip structure and relatively smooth surface due to solid phase melting and metaplast formation during the BC pyrolysis. The SD semi-coke particle exhibits rod morphology. The co-pyrolysis semicoke samples transformed from a strip structure to irregular granular shape as the SD percentage increases from 0% to 20 wt%. The above phenomena may be caused by the rapid volatile release of the SD during the co-pyrolysis process, which resulted in surface ablation and particle non-agglomeration observed on the co-pyrolysis semicoke surface.

4. Conclusions

In this paper, the chemical structure transformation as well as the gas evolution profiles during sawdust (SD)/coal blending (BC) co-coking are investigated using in-situ Fourier transform infrared

Please cite this article as: L. Qin et al., Synergistic effect for co-coking of sawdust and coal blending based on the chemical structure transformation, Journal of the Energy Institute, https://doi.org/10.1016/j.joei.2020.06.003

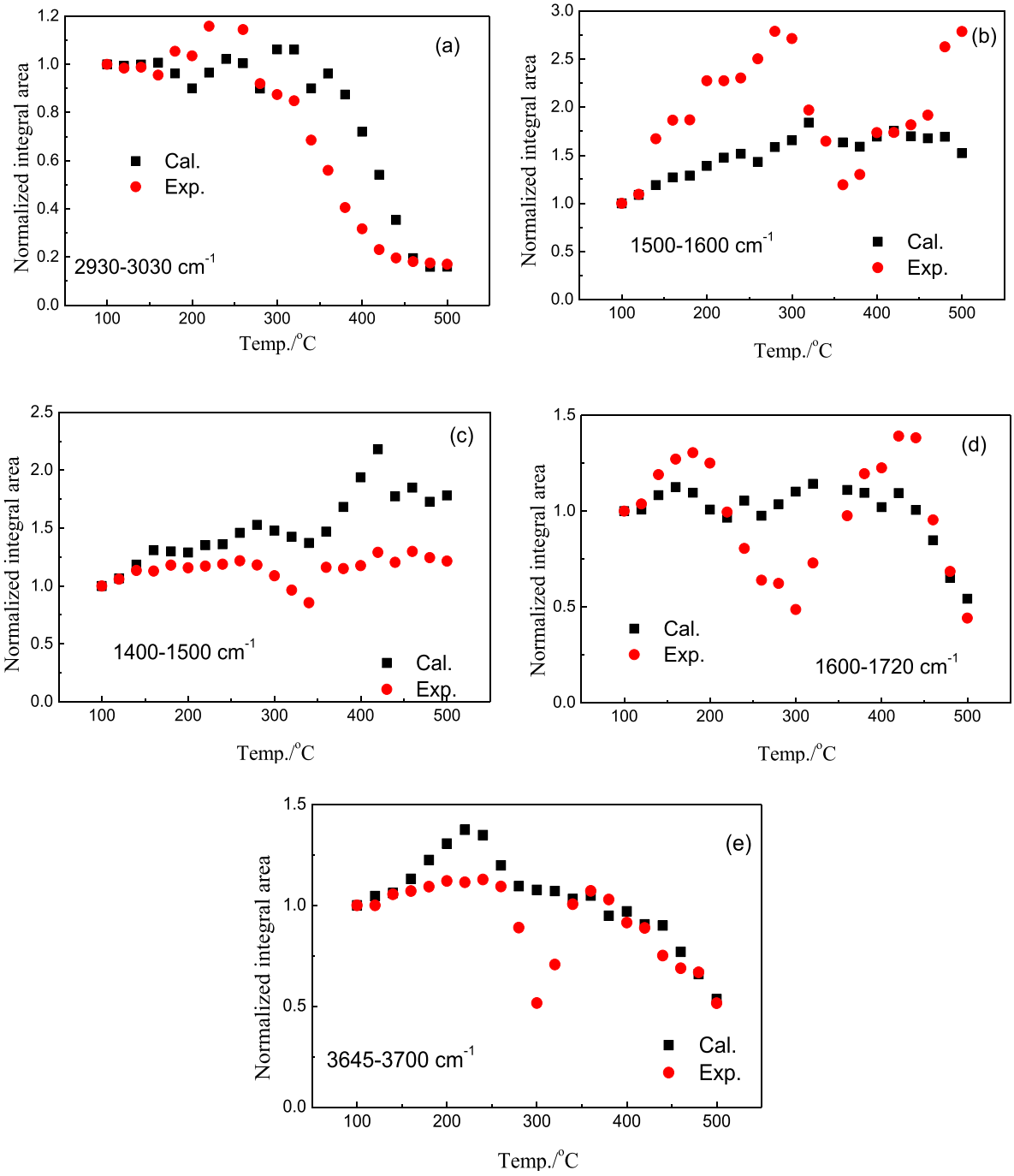

Fig. 8. The functional groups varied with the temperature between the experimental and the calculated results during the SDBC-20 blends co-pyrolysis.

spectroscopy coupled with mass spectrometry (In-situ FTIR-MS). Meanwhile, the role of sawdust in the semicoke formation is also studied by the Gieseler plastometer and scanning electron microscopy (SEM). The following conclusions have been obtained.

(1) The evolutions of the chemical structure between SD and BC exhibit the largest difference due to different structure. Different stages in various temperature ranges based on the chemical structure transformation and gas evolution are proposed for the individual SD/BC pyrolysis.

(2) The chemical structure transformation as well as the gas evolution profiles between experimental and the theoretical results are greatly different, which proves that the synergistic effect exists during the SD/BC blends co-pyrolysis.

(3) The synergistic effect caused by two stages during semicoke formation process. One stage (occurs at 100–280 °C) is caused by the physical effect. Another stage (happens at 280–500 °C) is mainly assigned to the hydrogen transfer.

(4) The thermoplastic properties decrease proportionately to the quantity of the SD and the non-agglomeration between BC and SD is clearly observed by SEM.

Please cite this article as: L. Qin et al., Synergistic effect for co-coking of sawdust and coal blending based on the chemical structure transformation, Journal of the Energy Institute, https://doi.org/10.1016/j.joei.2020.06.003

Acknowledgements

The present work is supported by National Natural Science Foundation of China (Grant No. 51706160), Hubei Technological Innovation Special Fund (Grant Nos. 2019ACA157, 2019AHB073 & 2019ZYYD060), and Foundation for Outstanding Youth Innovative Research Groups of Higher Education Institution in Hubei Province (T201902).

Appendix A. Supplementary data

Supplementary data to this article can be found online at https://doi.org/10.1016/j.joei.2020.06.003.

References

[1] T. MacPhee, L. Giroux, K.W. Ng, T. Todoschuk, M. Conejeros, C. Kolijn, Small scale determination of metallurgical coke CSR, Fuel 114 (2013) 229–234.
[2] S. Kudo, A. Mori, R. Soejima, F. Murayama, Karnowo, S. Nomura, Y. Dohi, K. Norinaga, J.-i. Hayashi, Preparation of coke from hydrothermally treated biomass in sequence of hot briquetting and carbonization, ISIJ Int. 54 (2014) 2461–2469.
[3] L. Qin, J. Han, W. Ye, S. Zhang, Q. Yan, F. Yu, Characteristics of coal and pine sawdust Co-carbonization, Energy Fuel. 28 (2014) 848–857.
[4] J.A. MacPhee, J.F. Gransden, L. Giroux, J.T. Price, Possible CO_2 mitigation via addition of charcoal to coking coal blends, Fuel Process. Technol. 90 (2009) 16–20.
[5] M.G. Montiano, E. Díaz-Faes, C. Barriocanal, R. Alvarez, Influence of biomass on metallurgical coke quality, Fuel 116 (2014) 175–182.
[6] E. Mousa, C. Wang, J. Riesbeck, M. Larsson, Biomass applications in iron and steel industry: an overview of challenges and opportunities, Renew. Sustain. Energy Rev. 65 (2016) 1247–1266.
[7] K.W. Ng, J.A. MacPhee, L. Giroux, T. Todoschuk, Reactivity of bio-coke with CO2, Fuel Process. Technol. 92 (2011) 801–804.
[8] M.G. Montiano, E. Díaz-Faes, C. Barriocanal, Partial briquetting vs direct addition of biomass in coking blends, Fuel 137 (2014) 313–320.
[9] S. Nomura, Recent developments in cokemaking technologies in Japan, Fuel Process. Technol. 159 (2017) 1–8.
[10] J. Rizkiana, G. Guan, W.B. Widayatno, X. Hao, W. Huang, A. Tsutsumi, A. Abudula, Effect of biomass type on the performance of cogasification of low rank coal with biomass at relatively low temperatures, Fuel 134 (2014) 414–419.
[11] H. Suopajärvi, K. Umeki, E. Mousa, A. Hedayati, H. Romar, A. Kemppainen, C. Wang, A. Phounglamcheik, S. Tuomikoski, N. Norberg, A. Andefors, M. Öhman, U. Lassi, T. Fabritius, Use of biomass in integrated steelmaking – status quo, future needs and comparison to other low-CO 2 steel production technologies, Appl. Energy 213 (2018) 384–407.
[12] H. Wang, W. Zhao, M. Chu, Z. Liu, J. Tang, Z. Ying, Effects of coal and iron ore blending on metallurgical properties of iron coke hot briquette, Powder Technol. 328 (2018) 318–328.
[13] X. Xing, H. Rogers, G. Zhang, K. Hockings, P. Zulli, A. Deev, J. Mathieson, O. Ostrovski, Effect of charcoal addition on the properties of a coke subjected to simulated blast furnace conditions, Fuel Process. Technol. 157 (2017) 42–51.
[14] Z.-R. Yang, Q.-Y. Meng, J.-J. Huang, Z.-Q. Wang, C.-Y. Li, Y.-T. Fang, A particle-size regulated approach to producing high strength gasification-coke by blending a larger proportion of long flame coal, Fuel Process. Technol. 177 (2018) 101–108.
[15] L. Florentino-Madiedo, D. Casal, E. Díaz-Faes, C. Barriocanal, Effect of sawdust addition on coking pressure produced by two low vol bituminous coals, J. Anal. Appl. Pyrol. 127 (2017) 369–376.
[16] B.D. Flores, I.V. Flores, A. Guerrero, D.R. Orellana, J.G. Pohlmann, M.A. Diez, A.G. Borrego, E. Osório, A.C.F. Vilela, Effect of charcoal blending with a vitrinite rich coking coal on coke reactivity, Fuel Process. Technol. 155 (2017) 97–105.
[17] A. Guerrero, M.A. Diez, A.G. Borrego, Influence of charcoal fines on the thermoplastic properties of coking coals and the optical properties of the semi-coke, Int. J. Coal Geol. 147–148 (2015) 105–114.
[18] E.M.A. Edreis, X. Lia, G. Luo, S.W. Sharshir, H. Yao, Kinetic analyses and synergistic effects of CO2 co-gasification of low sulphur petroleum coke and biomass wastes, Bioresour. Technol. 267 (2018) 54–62.
[19] D. Lv, M. Xu, X. Liu, Z. Zhan, Z. Li, H. Yao, Effect of cellulose, lignin, alkali and alkaline earth metallic species on biomass pyrolysis and gasification, Fuel Process. Technol. 91 (2010) 903–909.
[20] Z. Wu, Y. Li, B. Zhang, W. Yang, B. Yang, Co-pyrolysis behavior of microalgae biomass and low-rank coal: kinetic analysis of the main volatile products, Bioresour. Technol. 271 (2019) 202–209.
[21] P.R. Solomon, D.G. Hamblen, Understanding coal using thermal decomposition and fourier transform infrared spectroscopy, Am. Inst. Phys. 70 (1981) 121–140.
[22] P.R. Solomon, D.G. Hamblen, Finging order in coal pyrolysis kinetics, Prog. Energy Combust. Sci. 9 (1983) 323–362.
[23] P.R. Solomon, M.A. Serio, E.M. Suuberg, Coal pyrolysis: experiments, kinetic rates and mechanisms, Prog. Energy Combust. Sci. 18 (1992) 133–140.
[24] Z. Niu, G. Liu, H. Yin, C. Zhou, Devolatilization behaviour and pyrolysis kinetics of coking coal based on the evolution of functional groups, J. Anal. Appl. Pyrol. 134 (2018) 351–361.
[25] J. Han, W. Li, D. Liu, L. Qin, W. Chen, F. Xing, Pyrolysis characteristic and mechanism of waste tyre: a thermogravimetry-mass spectrometry analysis, J. Anal. Appl. Pyrol. 129 (2018) 1–5.
[26] L. Qin, J. Han, B. Zhao, Y. Wang, W. Chen, F. Xing, Thermal degradation of medical plastic waste by in-situ FTIR, TG-MS and TG-GC/MS coupled analyses, J. Anal. Appl. Pyrol. 136 (2018) 132–145.
[27] Z. Wu, W. Yang, X. Tian, B. Yang, Synergistic effects from co-pyrolysis of low-rank coal and model components of microalgae biomass, Energy Convers. Manag. 135 (2017) 212–225.
[28] X. Zhang, W. Yang, W. Blasiak, Modeling study of woody biomass: interactions of cellulose, Hemicell. Lig. Energy Fuel. 25 (2011) 4786–4795.
[29] Y. Zhang, Y. Zheng, M. Yang, Y. Song, Effect of fuel origin on synergy during co-gasification of biomass and coal in CO2, Bioresour. Technol. 200 (2016) 789–794.
[30] G.-M. Kim, K.Y. Lisandy, Y.Y. Isworo, J.-H. Kim, C.-H. Jeon, Investigation into the effects of ash-free coal binder and torrefied biomass addition on coke strength and reactivity, Fuel 212 (2018) 487–497.
[31] Z. Niu, G. Liu, H. Yin, D. Wu, C. Zhou, Investigation of mechanism and kinetics of non-isothermal low temperature pyrolysis of perhydrous bituminous coal by in-situ FTIR, Fuel 172 (2016) 1–10.
[32] M. Uchimiya, A. Orlov, G. Ramakrishnan, K. Sistani, In situ and ex situ spectroscopic monitoring of biochar's surface functional groups, J. Anal. Appl. Pyrol. 102 (2013) 53–59.
[33] E. Leng, Y. Zhang, Y. Peng, X. Gong, M. Mao, X. Li, Y. Yu, In situ structural changes of crystalline and amorphous cellulose during slow pyrolysis at low temperatures, Fuel 216 (2018) 313–321.
[34] S. Xin, H. Yang, Y. Chen, M. Yang, L. Chen, X. Wang, H. Chen, Chemical structure evolution of char during the pyrolysis of cellulose, J. Anal. Appl. Pyrol. 116 (2015) 263–271.
[35] C. Larabi, W.a. Maksoud, K.C. Szeto, O. Boyron, A. Roubaud, P. Castelli, C.C. Santini, J.J. Walter, Monitoring pine wood thermolysis under hydrogen atmosphere by in situ and ex situ techniques, J. Anal. Appl. Pyrol. 100 (2013) 81–87.
[36] X. Gu, X. Ma, L. Li, C. Liu, K. Cheng, Z. Li, Pyrolysis of poplar wood sawdust by TG-FTIR and Py–GC/MS, J. Anal. Appl. Pyrol. 102 (2013) 16–23.
[37] C. Liu, J. Hu, H. Zhang, R. Xiao, Thermal conversion of lignin to phenols: relevance between chemical structure and pyrolysis behaviors, Fuel 182 (2016) 864–870.
[38] Y. Zhang, J. Wang, S. Xue, J. Wu, L. Chang, Z. Li, Kinetic study on changes in methyl and methylene groups during low-temperature oxidation of coal via in-situ FTIR, Int. J. Coal Geol. 154–155 (2016) 155–164.
[39] G. Xiong, Y. Li, L. Jin, H. Hu, In situ FT-IR spectroscopic studies on thermal decomposition of the weak covalent bonds of brown coal, J. Anal. Appl. Pyrol. 115 (2015) 262–267.
[40] X. Li, Z.-h. Qin, L.-h. Bu, Z. Yang, C.-y. Shen, Structural analysis of functional group and mechanism investigation of caking property of coking coal, J. Fuel Chem. Technol. 44 (2016) 385–393.
[41] L. Vivero, C. Barriocanal, R. Álvarez, M.A. Díez, Effects of plastic wastes on coal pyrolysis behaviour and the structure of semicokes, J. Anal. Appl. Pyrol. 74 (2005) 327–336.
[42] W. Li, Z.-q. Bai, J. Bai, Z.-x. Guo, Decomposition kinetics of hydrogen bonds in coal by a new method of in-situ diffuse reflectance FT-IR, J. Fuel Chem. Technol. 39 (2011) 321–327.
[43] P. Giudicianni, G. Cardone, R. Ragucci, Cellulose, hemicellulose and lignin slow steam pyrolysis: thermal decomposition of biomass components mixtures, J. Anal. Appl. Pyrol. 100 (2013) 213–222.
[44] K. Kirtania, J. Tanner, K.B. Kabir, S. Rajendran, S. Bhattacharya, In situ synchrotron IR study relating temperature and heating rate to surface functional group changes in biomass, Bioresour. Technol. 151 (2014) 36–42.
[45] H.-m. Fang, J. Han, H.-j. Zhang, B. Zhao, L.-b. Qin, Effect of coal moisture content on coke's quality and yields of products during coal carbonization, J. Cent. S. Univ. 26 (2020) 3225–3237.
[46] K. Shi, J.M. Oladejo, J. Yan, T. Wu, Investigation on the interactions among lignocellulosic constituents and minerals of biomass and their influences on co-firing, Energy 179 (2019) 129–137.
[47] Z. Wu, S. Wang, J. Zhao, L. Chen, H. Meng, Synergistic effect on thermal behavior during co-pyrolysis of lignocellulosic biomass model components blend with bituminous coal, Bioresour. Technol. 169 (2014) 220–228.
[48] Z.-S. Niu, Y.-G. Wang, J. Shen, Y.-X. Niu, G. Liu, W. Zhao, X.-Y. Wei, Insight into aromatic structures of a middle-temperature coal tar pitch by direct characterization and ruthenium ion-catalyzed oxidation, Fuel 241 (2019) 1164–1171.
[49] Z. Ma, Y. Yang, Y. Wu, J. Xu, H. Peng, X. Liu, W. Zhang, S. Wang, In-depth comparison of the physicochemical characteristics of bio-char derived from biomass pseudo components: hemicellulose, cellulose, and lignin, J. Anal. Appl. Pyrol. 140 (2019) 195–204.
[50] L. Qin, X. Huang, B. Zhao, Y. Wang, J. Han, iron oxide as a promoter for toluene catalytic oxidation over Fe–Mn/γ-Al_2O_3 catalysts, Catal. Lett. 150 (2019) 802–814.

Please cite this article as: L. Qin et al., Synergistic effect for co-coking of sawdust and coal blending based on the chemical structure transformation, Journal of the Energy Institute, https://doi.org/10.1016/j.joei.2020.06.003

[51] Z. Wu, C. Ma, Z. Jiang, Z. Luo, Structure evolution and gasification characteristic analysis on co-pyrolysis char from lignocellulosic biomass and two ranks of coal: effect of wheat straw, Fuel 239 (2019) 180–190.
[52] L. Florentino-Madiedo, E. Díaz-Faes, C. Barriocanal, Mechanical strength of bio-coke from briquettes, Renew. Energy 146 (2020) 1717–1724.
[53] A.M. Parvez, T. Wu, Y. Hong, W. Chen, E.H. Lester, S. Mareta, M. Afzal, Gasification reactivity and synergistic effect of conventional and microwave pyrolysis derived algae chars in CO2 atmosphere, J. Energy Inst. 92 (2019) 730–740.
[54] X. Zhu, X. Li, L. Xiao, X. Zhang, S. Tong, C. Wu, R. Ashida, W. Liu, K. Miura, H. Yao, Novel carbon-rich additives preparation by degradative solvent extraction of biomass wastes for coke-making, Bioresour. Technol. 207 (2016) 85–91.
[55] H. Cheng, S. Wu, J. Huang, X. Zhang, Direct evidence from in situ FTIR spectroscopy that o-quinonemethide is a key intermediate during the pyrolysis of guaiacol, Anal. Bioanal. Chem. 409 (2017) 2531–2537.
[56] J. Han, Y. Liang, J. Hu, L. Qin, J. Street, Y. Lu, F. Yu, Modeling downdraft biomass gasification process by restricting chemical reaction equilibrium with Aspen Plus, Energy Convers. Manag. 153 (2017) 641–648.
[57] Y. Lin, Y. Liao, Z. Yu, S. Fang, X. Ma, A study on co-pyrolysis of bagasse and sewage sludge using TG-FTIR and Py-GC/MS, Energy Convers. Manag. 151 (2017) 190–198.
[58] L. Luo, J. Liu, H. Zhang, J. Ma, X. Wang, X. Jiang, TG-MS-FTIR study on pyrolysis behavior of superfine pulverized coal, J. Anal. Appl. Pyrol. 128 (2017) 64–74.
[59] L. Qin, X. Huang, Q. Xue, L. Liu, Y. Wan, In-situ biodegradation of harmful pollutants in landfill by sludge modified biochar used as biocover, Environ. Pollut. 258 (2020), 113710.
[60] L. Qin, Z. Xu, L. Liu, H. Lu, Y. Wan, Q. Xue, In-situ biodegradation of volatile organic compounds in landfill by sewage sludge modified waste-char, Waste Manag. 105 (2020) 317–327.
[61] Q. Wang, D. Cui, P. Wang, J. Bai, Z. Wang, B. Liu, A comparison of the structures of >300 °C fractions in six Chinese shale oils obtained from different locations using 1H NMR, 13C NMR and FT-IR analyses, Fuel 211 (2018) 341–352.

Please cite this article as: L. Qin et al., Synergistic effect for co-coking of sawdust and coal blending based on the chemical structure transformation, Journal of the Energy Institute, https://doi.org/10.1016/j.joei.2020.06.003